NASA

Technical Memorandum 83914

On the Acceleration of Ions by Interplanetary Shock Waves: III High Time Resolution Observations of CIR Proton Events

M. E. Pesses, J. A. Van Allen,
B. T. Tsurutani, E. J. Smith

DECEMBER 1981

National Aeronautics and
Space Administration

Goddard Space Flight Center
Greenbelt, Maryland 20771

On the Acceleration of Ions by Interplanetary Shock Waves: III High Time Resolution Observations of CIR Proton Events

by

M.E. Pesses[1,2,4], J.A Van Allen[2],

B.T. Tsurutani[3], E.J. Smith[3]

[1] Laboratory for Astronomy and Solar Physics, Goddard Space Flight Center, Greenbelt, Maryland 20771

[2] Department of Physics and Astronomy, University of Iowa Iowa City, Iowa 52242

[3] Jet Propulsion Laboratory, Pasadena, California 91103

[4] National Academy of Sciences' National Research Council Fellow

April 1982

ABSTRACT

Observations within ± 3 hours of corotating interaction region (CIR) shock waves of proton intensities, pitch angle distribution and crude differential energy spectra of the range of $0.6 \leq E_p \leq 3.4$ MeV are presented. The principle result is the evidence for the persistent flow of particles away from the shock. The observations are found to be in good agreement with the hypothesis of local interplanetary shock acceleration by the shock drift and compression mechanisms. The same set of observations strongly suggests that transit time damping does not play an important role in the acceleration of protons to 1 MeV in the immediate vicinity of CIR shocks.

I. INTRODUCTION

The first observations in space of interplanetary shock associated enhancements in the intensity of energetic protons were those of Van Allen and Whelpley [1962] with Injun 1 and Explorer 12 and of Bryant et al. [1962] with Explorer 12.

Since then two distinct types of interplanetary shock wave associated proton intensity enhancements are observed at and inside the earth's orbit (1 AU).

The most frequently observed type of enhancement is called a shock spike event or low-energy (~ 0.3 - 10 MeV/nucleon) energetic storm particle event (LESP) [Axford and Reid, 1963; Van Allen and Ness, 1967; Armstrong et al., 1970; Lanzerotti and Soltiz, 1970; Singer, 1970; Ogilvie and Arenes, 1971; Palmeria et al., 1971; Palmeria and Allum, 1973; Armstrong and Krimigis, 1973; Sarris and Van Allen, 1974; Sarris et al., 1975, 1976]. The enhancements exhibit a slow rise in intensity a few minutes before shock passage a very rapid rise to maximum at ~ ± 1 min of the time the shock is observed, and a rapid decay. Multi-spacecraft observations show that the intensity peak moves with the shock front [Palmeria and Allum, 1973]. Strong anisotropies directed away from the sun are frequently observed. The energy spectrum of the protons in the "spike" is softer than that of the ambient population.

Less frequently observed than shock spike events are energetic storm particle events (ESP) [Van Allen and Whelpley, 1962; Bryant et al., 1962; Rao et al., 1967; Singer, 1970; Vernov et al., 1967; Palmeria et al., 1971; Sarris, 1973; Gosling et al., 1980]. ESP events are observed during the decay stage of solar flare proton events, are temporally associated with a shock wave from the flare site, and usually have an observed energy range $0.01 \lesssim E \lesssim 45$ MeV/nucleon. The shock associated increase in intensity observed by earth-orbiting satellites

begins several hours before the passage of a shock wave or the detection of a strong sudden commencements (SSC). (SSC usually signals the collision of a shock wave with the earth's magnetosphere.) ESP events last ~ 6 hours, have a softer spectrum than that of the ambient proton population (but a harder spectrum than do shock spike events), and contain period of strongly anisotropic fluxes. ESP events decay abruptly and are usually followed by Forbush decreases. Bidirectional anisotropies are commonly observed at the cessation of the events.

Enhancements in the intensity of alpha particles and ions with Z up to 26 have been observed in ESP and LESP events [Armstrong and Krimigis, 1973; Sarris et al., 1976]. Enhancements in the He, C and O have been observed by Hamilton et al. [1979] in corotating interaction region events. Electron enhancements associated with interplanetary shock waves have also been reported [Armstrong and Krimigis, 1976; Pesses, 1976; Potter, 1981].

Observations out to 20 AU from the sun of shock associated proton intensity enhancements have been made by Pioneers 10 and 11 and Voyagers 1 and 2 [Barnes and Simpson, 1976; McDonald et al., 1976, 1981; Pesses et al., 1978, 1979; Hamilton et al., 1979; Van Hollebeke et al., 1979; Tsurutani et al., 1981; Decker et al., 1981]. Some deep space shock events apparently extend back to 1 AU where they have been observed by Gloeckler et al. [1979] (and references therein).

The deep space events have been observed over an energy range of 30 keV $\lesssim$ Ep $\lesssim$ 20 MeV. The duration of the deep space events is ~ 1 - 5 days, and the peak intensity at ~ 1 MeV in protons $(cm^2\ s\ sr\ MeV)^{-1}$ is ~ 1/10 - 1/100 of that of ESP and LESP events. However, the peak to background ratios of the deep space events ~ 1 MeV protons are ~ 10^2 - 10^3 as compared with ~ 10^1 - 10^2 for most the 1 AU events. The distribution function of the deep space events closely

resembles an exponential function in velocity or momentum [Gloeckler et al., 1979; Mewaltt et al., 1980; Van Hollebeke et al., 1979].

The purpose of this paper is to compare the predictions of acceleration by shock drift and compression mechanisms with the fine scale feature of deep space shock associated energetic particle events. This particular model of shock acceleration is presented in two companion papers [Pesses, 1982; Pesses and Decker, 1982].

II. THE EXPERIMENT

The University of Iowa instrument aboard Pioneer 11 has been described previously by Pesses et al. [1978]. The magnetometer aboard Pioneer 11, which was used in this study, is the Jet Propulsion Laboratory vector helium magnetometer and has been previously described [Smith et al., 1975]. The Ames Research Center (ARC) plasma analyzer experiment aboard Pioneer 11 is identical to the ARC plasma experiment aboard Pioneer 10 [Wolfe et al., 1974].

A. Angular Distributions

The rotational axis of Pioneer 11 is pointed continuously at earth with an error of less than 1° and therefore lies approximately in the ecliptic plane. The rotational period is measured accurately and continuously and during the period to be investigated is about 12.5 s.

The pitch angle of particles being observed depends on the roll angle ϕ of the detector and the angle θ_B between the local interplanetary magnetic field vector $\vec{B}$, and the spacecraft spin-axis. For a given value of θ_B the pitch angle α being sampled as a function of the angle ϕ is given by Equation (1),

$$\cos \alpha = - \sin \theta_B \cos(\phi - \phi_B) \qquad (1)$$

In equation (1) ϕ is the roll angle of the detector axis measured from the ascending node of the spacecraft equatorial plane on the ecliptic, and ϕ_B is the "roll angle" of the projection of $\vec{B}$ onto the spin plane of the detectors. The minimum and maximum pitch angles sampled are $(90° - \theta'_B)$ and $(90° + \theta'_B)$, respectively, where θ'_B is the acute value of θ_B.

Temporal variations in the direction of $\vec{B}$, and hence the value of θ'_B result in a variability of the range of pitch angle observed. This results in pitch angles near 90° being sampled more frequently than pitch angles near either 0° or 180°. To compensate for this effect, pitch angles are divided into three sectors, S_1 (α =0° - 60°), S_2 (α = 61° - 120°), and S_3 (α =121° - 180°). The counting rates observed in each individual sector are fit to a first order Fournier expression of the form

$$j(\alpha) = J[(1 + K \cos(\alpha - \Delta)] \qquad (2)$$

where $j(\alpha)$ is the counting rate measured at α, J the spin averaged counting rate, K the anisotropy amplitude and Δ the anisotropy direction. The dependence of J, K and Δ on the counting rates of sectors S_1, S_2 and S_3 is given in Equations (3a - 3c).

$$J = \frac{S_1 + S_2 + S_3}{3} \qquad (3a)$$

$$K = \frac{\sqrt{\left(\frac{S_1 - S_3}{3}\right)^2 + \left(\frac{S_1 - 2S_2 + S_3}{9}\right)^2}}{S_1 + S_2 + S_3} \qquad (3b)$$

$$\Delta = \cos^{-1}\left[\frac{S_1 - S_3}{\left[(S_1^2 - S_3^2) + \left(\frac{S_1 - 2S_2 + S_3}{3}\right)^2\right]^{1/2}}\right] \qquad (3c)$$

The pitch angle distributions to be presented in this paper are averaged over one hour and represent a superposition of one-minute average distributions which are constructed using one-minute averages of the interplanetary magnetic field (IMF) $\vec{B}$ [variable in both direction and magnitude] and a particle counting rate [which is telemetry bit-rate-dependent] of 0.1875 to 1.5 secs. The values of α used in both the pitch angle distributions and least-squares anisotropy fits are those for the center of the detector at the midpoint of the sampling period.

If the pitch angle distribution is anisotropic the direccion of the particle flow with respect to the shock front is determined by examining the average polarity of the upstream and downstream magnetic field during the period for which the pitch angle distribution is constructed. If the polarity is negative ($\vec{B}$ directed towards the sun) particles with $0° \leq \alpha \leq 90°$ are considered to be flowing inward toward the sun and particles with $90° < \alpha \leq 180°$ are considered to be flowing outward, away from the sun. If the polarity is positive ($\vec{B}$ directed away from the sun) particles with $180° \leq \alpha \leq 90°$ are considered to be flowing inward toward the sun and particles with $90° < \alpha \leq 0°$ are considered to be flowing outward, away from the sun. For a reverse (forward) shock the upstream flow is away from the shock if the flow is toward (away) from the sun and toward the shock if the flow is away from (toward) the sun. For a reverse (forward) shock the downstream flow is away from the shock if the flow is away (toward) the sun, and toward the shock if the flow is toward (away) from the sun.

The Compton-Getting effect on the anisotropies of 0.61 MeV protons in regions of high solar wind velocity can be significant. For a solar wind speed equal to 550 km s^{-1} and a proton differential power spectral index γ in the solar wind rest frame of 3, the convective anisotropy k' measured in the

ecliptic plane is 0.33 [Forman, 1970]. The spin plane of the detector (G) making the measurements is, however, perpendicular to the earth-spacecraft line plus or minus 1°. The Compton-Getting anisotropy direction is radially away from the sun along the sun-spacecraft line. Hence, k", the component of the Compton-Getting anisotropy that is measured in the spin plane, is k' sin β where β is the sun-spacecraft-earth angle ($|\beta| \approx 15°$) and $k'' < 0.1$. None of the pitch angle distributions to be presented have been corrected for the Compton-Getting effect.

B. Energy Spectra

If no electrons with $E_e > 0.047$ MeV are present and if the counting rate of detector G due to protons is much greater than the counting rate due to alpha particles and ions $Z > 3$, the ratio of the counting rate of G to the difference of the counting rates of detectors A and C is a measure of the proton energy spectrum (cf. Table 1). For a spectrum of the form

$$j(v)dv = \tilde{K}\, e^{-v/vo}dv \qquad (4)$$

where j(v)dv is the intensity of protons with speed between v and v + dv, $\tilde{K}$ is a constant, and vo is the e-folding speed

$$vo = \frac{14800 \text{ km s}^{-1}}{|\ln(1 - 0.486G^*)|} \qquad (5)$$

$$G^* = \frac{G}{A - C} \qquad (6)$$

and G, A, and C are counting rates of detectors G, A, and C, respectively. In formula (6) it is understood that the calibration source rate has been subtracted from the raw rate of G; and further that the rate of C has been multipled by an empirical factor of about 1.08 determined in flight so as to make the galactic

cosmic ray rates of A and C equal. In graphs and other presentations of data, this directly measured parameter G*, rather than the more meaningful parameter vo, has been preferred because of possible contributions of electrons to the counting rate (A - C), a matter requiring auxiliary consideration. Values of G* < 1.5 are probably the result of electron contamination in the Geiger tube detector A combing rate.

III. OBSERVATIONS OF THE FINE SCALE FEATURES OF SHOCK-ASSOCIATED ENERGETIC PARTICLE EVENTS

A. General Considerations

Figure 1 gives a schematic view of the shock acceleration - spacecraft observation process. The thick curves line at the bottom of the figure is a shock wave. The wavy lines represent IMF lines. The vertical line shows the spacecraft's relative path through the solar wind convected IMF

At various distances (A, B, C) from the shock, the spacecraft is magnetically connected at different locations along the shock front (a, b, c).

The pre-interaction charged particle population is accelerated at and in the vicinity of the shock front. The obliqueness and magnetic shock strength are possibly functions of position due to spatial variations in the IMF. The particles are accelerated at or near the shock front, and then propagate away from the shock via convection and diffusion.

Between leaving the vicinity of the shock front and being observed, the particle's pitch angle changes due to scattering off of IMF irregularities.

Because the pitch angle distribution of accelerated particles and the shock conditions under which the particles were accelerated can vary along the space-

craft path we analyze those data taken only in the immediate vicinity of the shock and assume that variations along the shock front are minimal.

B. Fine Time Scale Study of CIR Shock Associated EPE (Pioneer 11)

In this section a fine time scale (1 - 10 min) study of a sample of counting interaction region (CIR) shock associated energetic proton events (EPE) is carried out.

The events are presented graphically in two types of figures. In one type, Figure a's, going from the top to bottom panel, are: One minute averages of the IMF $|\vec{B}|$; $|90 - \psi_R|$ where ψ_R is the reconstructed value of ψ_1 (the angle between the shock normal and the upstream magnetic field vector); one minute averages of the counting rate of detector G ($0.6 \leq E_p \leq 3.4$ MeV) with standard deviation error bars plotted every other minute; and ten minute averages of the detector G anisotropy amplitude K, anisotropy direction Δ, and the detector ratio G*, respectively. The data are presented for $\pm$ 3 hr from the time of shock passage except if data gaps occur.

In the other type, Figure b's, 1 hour average pitch angle distributions are presented with upstream (downstream) distribution on the top (bottom). The number in the upper left corner of each panel refers to the temporal order of the observations. For example, for forward (reverse) shocks, panel 3 is the distribution compiled over the period immediately 1 hour upstream (downstream) of the shock front. The data are presented so that a particle with a pitch angle plotted to the left (right) of 90° is directed toward (away) from the shock front. The sun symbol o indicates the direction of sunward flow.

The reconstructed values of ψ_1, ψ_R is calculated using the observed shock normal direction $\hat{n}$, and the following simplifying assumptions:

1) $\hat{n}$ does not change along the shock front or with time;

2) the magnetic shock strength N does not change along the shock front or with time; and

3) the direction and magnitude of $\vec{B}$ do not change after passing through the shock front.

Using the fact that the component of $\vec{B}$ normal to the shock surface is continuous across the shock front (i.e., $\hat{n} \cdot \vec{B}_1 = \hat{n} \cdot \vec{B}_2$), where $\vec{B}_1$ ($\vec{B}_2$) is the upstream (downstream) magnetic vector, the coplanarity theorem gives

$$\cos \psi_1 = \frac{\hat{n} \cdot \vec{B}_1}{|\vec{B}_1|} = \frac{\hat{n} \cdot \vec{B}_2}{|\vec{B}_2|/N}$$

and $\cos \psi_1 = N \cos \psi_2$, and $N = |\vec{B}_2|/|\vec{B}_1|$.

Thus

$$\psi_R = \cos^{-1}(N \cos \psi_2) \quad . \tag{7}$$

An assumption number (3) is not always a good one, the absolute value of the argument of the arc cosine in Equation (7) can sometimes exceed 1. In these cases ψ_R is set = 0°.

Five of the six shocks present here are of the reverse type. This is because the ~ 1 MeV proton intensity of the CIR shock associated events are significantly larger at reverse shocks, than forward shocks.

1. DOY 238/1973

This event has been discussed previously by Pesses et al. [1979]. Figure 2(a) gives the high resolution data, Figure 2(b) the pitch angle distributions. The upstream flow is directed away from the reverse shock and toward the sun,

with the maximum proton intensity at (α max) $\approx 150°$ and $K \approx 0.4$. The field aligned sunward flow of the upstream protons is very difficult to explain by the mirroring of solar flare protons as that process would produce a pitch angle distribution $\approx$ symmetric about 90°. The sunward flow of protons also cannot be attributed to the solar wind Compton Getting effect as the solar wind convective anisotropy is radially outward from the sun.

The downstream flow is directed away from the shock and outward from the sun with $90° < \alpha$ max $< 110°$ with an average K value of 0.25. The observed pitch angle distributions are consistent with Pesses' and Decker's [1981] mode II acceleration. The proton counting rate decreases by 10 s^{-1} simultaneously with the passage of the reverse shock at 0742 UT. Notice how the anisotropy direction Δ also changes by 150° from antisunward to sunward at this time. The downstream energy spectrum is slightly harder than the upstream spectrum. Spike-like counting rate enhancements of $\sim$ 10 minutes in duration peaking at 0555 UT, 0615 UT and 0638 UT occur within one minute when the reconstructed shock geometry is nearly perpendicular and in between periods when $\psi_R \sim 0°$.

Shock acceleration is most intense when the shock is nearly perpendicular ($90° < \psi_1 < 82°$) after a period when the shock was quasi-parallel. [Pesses and Decker, 1982]. The post-interaction counting rates will be the highest along those field lines that are nearly perpendicular to $\hat{n}$. As the shock propagates through the upstream plasma, these highly populated field lines are left downstream of the shock front, and eventually convected past the spacecraft by the solar wind. Whether or not particle intensity enhancements are observed when $\psi_R \sim 90°$ depends on the accuracy of the assumptions by which the values of ψ_1 are reconstructed (which probably varies from shock to shock), the number of particles available for acceleration and how long the accelerated particles remain on the "nearly perpendicular" field lines.

The length of time during which the "nearly perpendicular" downstream field lines will be associated with observable proton intensity enhancements depends on the length of the field line along which the shock acceleration occurs and on the local diffusion coefficient. For scatter-free propagation, and for 1 MeV protons with an average pitch angle of 60° on a field line observed 2 hr from shock passage, an acceleration region of ~ 0.17 AU in length is needed. Pitch angle scattering will increase the time protons spend on the "nearly perpendicular" field lines and shortens the acceleration region length required. Cross field diffusion will increase both the length of the required acceleration region and the observed spatial extent of the intensity enhancements. The observation of proton "enriched", nearly perpendicualr field lines is consistent with Pesses and Deckers' [1982] mode II acceleration.

2. DOY 163/1973

Figure 3(a) gives the high resolution data, Figure 3(b) the pitch angle distributions. The upstream energetic proton flow is away from the reverse shock and toward the sun, with maximum proton intensity observed at $\alpha \sim 50°$ and with $K \sim 0.45$. This is consistent with mode II acceleration. The downstream flow is isotropic, except between 11 - 12 UT, panel 1, where it is directed toward the shock and toward the sun with $K \sim 0.25$. The downstream distribution suggests that the diffusion coefficient is smaller downstream than upstream. The upstream intensity is a factor of 2 greater than the downstream intensity. The passage of the shock at 1315 UT coincides to 1 minute with a 11 s^{-1} counting rate decrease. The energy spectrum is softest ± one-half hour from the time the shock is observed.

3. DOY 103/1974

Figure 4(a) presents the high resolution data, Figure 4(b) the pitch angle distributions. The upstream flow is bidirectional immediately upstream in panel 4, then farther from the shock the flow is directed away from the shock and towards the sun with α max $\approx$ 55° and K ~ 0.2. The downstream pitch angle distribution is pancake in panel 3, peaked perpendicular to the field in panel 2 and field aligned and directed away from the shock and the sun in panel 1. The intensity decreases by a factor of 2 at the time of shock passage. There is some correlation between periods of ψ_R ~ 80° and factors of 2 increase in the intensity at around 0140 UT and 0210 UT. Event 3 is constant with mode III acceleration.

4. DOY 166/1974

The high resolution (pitch angle) data are presented in Figure 5(a) and 5(b). The flow immediately upstream of the forward shock (panel 3) is directed away from the shock and outward from the sun, with α max = 60° and K $\approx$ 0.2. The flow farther upstream (panels 1 and 2) is basically isotropic. The downstream flow has a small, net component which is directed away from the shock and inward toward the sun. A factor of 3 enhancement in the proton counting rate is observed one-half hour prior to the passage of the forward shock at 1831 UT. The pitch angle anisotropy goes from 135° to 45° during the course of the enhancement. Immediately downstream of the shock ψ_R ~ 80°. The upstream spectrum is hard with G* ~ 0.2. The small upstream K values and the small upstream values of G* and the upstream intensity peak suggest mode III or IV acceleration.

5. DOY 329/1973

The high resolution data for this event is presented in Figure 6(a). The pitch angle data are shown in Figure 6(b).

The flow of protons immediately upstream (panel 3) has a small net component away from the shock and inward toward the sun. The upstream flow then becomes isotropic (panel 4). The downstream flow is isotropic. The reconstructed shock geometry is nearly parellel between 4 and 5 UT and the average value of ψ_R is $\sim 45°$ around the time the shock is observed at 0715 UT. Neither proton intensity nor spectrum is apparently affected by the shock passage.

The calculated value of V_{1x}, the normal component of the shock's velocity in the upstream plasma rest frame for this event is 116 km x^{-1} and the observed value of N is 1.84. During 1973 and 1974 using Pioneer 11 data, the mean value of V_{1x} and N for those detector G enhancements that peak within ± 2 hr of a CIR shock [Pesses, (1976)] is 190 km s^{-1} and 2.1 respctively. The mean value of V_{1x} and N for those shocks for which there are V_{1x} data and for which Pesses [1976] observed no detector enhancements with peak intensity < 0.2 cs^{-1} on detector G is 94 km s^{-1} and 1.84 respectively. Hence, a V_{1x} of 116 km s^{-1} combined with $\psi_R \sim 45°$ would on the average be sufficient not to produce any noticeable changes in the proton intensity. The event is consistent with mode IV acceleration.

6. DOY 302/1974

Figure 7(a) and 7(b) presents the high resolution (pitch angle) data. The upstream flow is bidirectional and nearly symmetric about $\alpha = 90°$ for the period 0 - 3 hr from the reverse shock. The particle distribution is isotropic immediately downstream (panel 3), then switches to slightly anisotropic with a

net component away from the shock and outward from the sun. There is a ~ 20 minute intensity enhancement of ~ 50% at 0730 UT. The anisotropy amplitude goes 0.4 to 0.2 during the enhancement. The anisotropy direction goes from 40° to 120° at 0740 UT which is ~ 10 minutes after the decline of the intensity. The downstream intensity does not vary signifcantly even though $\psi_R \sim 80°$ on many occasions The energy spectrum remains very hard G ~ 0.1 throughout the event. The upstream pitch angle distributions are consistant with the mirroring of a vast majority of $0.6 \leq E_p \leq 3.4$ MeV protons by the shock. Using the observed value of N = 3.25 and calculated values of $\psi_1 \sim 80°$, the reflection coefficient for 1 MeV protons calculated from Pesses 1981 is 0.80 (0.77) for $V_{1x} = 190$ (300) km s^{-1}. While the mirroring of particles complicates matters, the upstream intensity peak, hard spectrum and no correlation between ψ_R and the downstream intenisty suggest mode IV acceleration.

V. CONCLUSIONS AND DISCUSSION

1. The observations presented here and those observations discussed in Pesses and Decker [1982] of ~ 1 MeV proton intensity, pitch and angle distribution and energy spectrum in the vicinity of CIR shocks are consistant with the predictions of the multiple encounter, shock drift and compression mechanisms. This conclusion is based on the following:

(a) Events 1 and 2 in this paper which exhibit the highest peak counting rates also exhibit the best correlation between downstream counting rate peaks and reconstructed values of ψ_1. Also, in these events the flow of particles away from the shock and the general shape of both upstream and downstream pitch angle distributions are the most consistent with the predictions of the single encounter theory. Events 1 and 2 are mode II in nature and the number (n) of times the

average particle encounters a shock is relatively small, which helps to preserve the large anisotropic single encounter features of the events.

(b) The observed functional forms of the particle distribution function is an exponential velocity or momentum is in good agreement with the predictions of Fisk and Lee (1980) and Pesses and Decker [1982].

(c) The observed value of the e-folding speed of the characteristic distribution function ~ 3000 km s^{-1} agrees with the Pesses and Decker [1982] predicted value when realistic values of V_{1x}, N and ψ_1 are used.

(d) The geometry of the IMF is such that the value of ψ_1 for reverse CIR shocks is expected to be larger than that of forward CIR shocks (cf. Figure 3) [Pesses, and Decker, 1982b]. Pesses and Decker [1982] predicts that this will result, on the average, in the energy spectrum being harder and peak to background values being larger for the reverse events than for the forward events. This predicted difference between the reverse and forward events has been observed by Barnes and Simpson [1976].

(e) The intensity, pitch angle distributions, and correlation between counting rate enhancements and reconstructed values of ψ_1 observed with ± 3 hr of CIR shocks are basically described by the multiple mode shock acceleration classification of Pesses and Decker [1982b].

(f) The species variation in the e-folding velocity observed by Mer ldt et al. [1979b] and McGuire et al. [1980] is consistent with that predicted by Pesses and Decker [1982].

2. The salient feature of the CIR shock associated events at ~ 1MeV/nucleon reported here are not explainable by transit time damping. This conclusion is based on the following:

(a) The transit time damping (TTD) acceleration model [Fisk, 1976] suggests

that the observed heliocentric radial gradient of the intensity of ~ 1 MeV protons can be accounted for if continuous TTD occurs from the solar corona to the point of observation. For a spacecraft at 4 AU where the largest event intensities are observed [Van Hollenbeke et al., 1978], the TTD acceleration process has been underway for ~ 2 weeks. This is inconsistent with the observation that the counting rate peaks move with the shock [Barnes and Simpson, 1976] and that with the positive correlation between peak event intensity and pitch angle anisotropy amplitude in Figures 2 - 7. A negative correlation between intensity and pitch angle anisotropy is expected for a stochastic process.

(b) The TTD model predicts field aligned anisotropies. Field aligned anisotropies are frequently observed upstream but only infrequently downstream of CIR shocks.

(c) The fine time (~ 1 minute) scale correlation observed between proton counting rate and fluctuations in ψ_1 is very difficult to explain if TTD is the dominant acceleration mechanism.

ACKNOWLEDGMENTS

This work at the University of Iowa was supported by contract NAS2-6553 with the Ames Research Center/NASA and the U.S. Office of Naval Research and at the Goddard Space Flight Center/NASA by the Laboratory for Astronomy and Solar Physics. This paper also includes results of one aspect of research done at the Jet Propulsion Laboratory, California Institute of Technology for the National Aeronautics and Space Administration under contract NAS7-100. M.E. Pesses is a National Academy of Sciences' National Research Council resident research associate at GSFC.

REFERENCES

Armstrong, T.P., and S.M. Krimigis, Time variations and angular distributions of alpha particles and medium nuclei for the October 29, 1972 solar particle event, a contribution to the 13th International Cosmic Ray Conference, Denver, Colorado, August 17-30, 1973.

Armstrong, T.P., and S.M. Krimigis, Interplanetary acceleration of relativistic electrons observed with Imp 7, J. Geophys. Res., 81, 677-682, 1976.

Armstrong, T.P., S.M. Krimigis, and K.W. Behannon, Proton fluxes at 300 keV associated with propagating interplanetary shock waves, J. Geophys. Res., 75, 5980-5988, 1970.

Axford, W.I., and G.C. Reid, Increases in intensity of solar cosmic rays before sudden commencements of geomagnetic storms, J. Geophys. Res., 68, 1973-1803, 1963.

Barnes, C.W., and J.A. Simpson, Evidence for interplanetary acceleration of nucleons in corotating interaction regions, Astrophys. J. Lett., 201, L91-L96, 1976.

Bryant, D.A., T.L. Cline, U.D. Desai, and F.B. McDonald, Explorer 12 observations of solar rays and energetic storm particles after solar flare of September 28, 1961, J. Geophys. Res., 67, 4893-5000, 1962.

Decker, R.B., M.E. Pesses, and S.T. Krimigis, Observations of shock associated low energy ions by Voyagers 1 and 2, in press, J. Geophys. Res., 1981.

Fisk, L.A., The acceleration of energetic particles in the interplanetary medium by transit time damping, J. Geophys. Res., 81, 4633-4640, 1976.

Fisk, L.A. and M.A. Lee, Shock acceleration of energetic particles in corotating interaction regions, Astrophys. J., 237, 620-624, 1980.

Forman M.A., The Compton-Getting effect for cosmic-ray particles and photons and the Lorentz-Invariance of distribution functions, Planet. Space Sci., 18, 25-31, 1970.

Gloeckler, G., D. Hovestadt, and L.A. Fisk, Observed distribution functions of H, H_e, C, O, and F_e in corotating energetic particle streams: Implications for interplanetary acceleration and propagation, Astrophys. J., 230, L191-L195, 1979.

Gosling, J.T., Asbridge, J.R., Bame, S.S, Feldman, W.C., Paschman, G. and Skopke, H., solarwind ions accelerated to 40 keV by shock wave disturbances, J. Geophys. Res., 85, 744-762, 1980.

Hamilton, D.C., G. Gleockler, T.P. Armstrong, W.J. Axford, C.O. Bostrom, C.Y. Fan, S.M. Krimigis, and L.J. Lanzerotti, Recurrent energetic particle events associated with forward/reverse shock pairs near 4 AU in 1978, Conference Papers, 16th International Cosmic Ray Conference, Kyoto, Japan.

Lanzerotti, L.J. and C.M. Soltis, Interplanetary protons and alphas: Days 300-313, 1968, World Data Center A Report UAG-8, 198-204, March 1970.

McDonald, F.B., B.J. Teegarden, J.H. Trainor, T.T. Von Rosenvinge, and W.R. Webber, The interplanetary acceleration of energetic nucleons, Astrophys. J. Lett., 203, L149-L153, 1976.

McDonald, F.B., T.H. Trainor, J.D. Minalow, J.H. Wolfe, W.R. Webber Radially propagating shock waves in the outer heliosphere: the evidence from Pioneer 10 energetic particle and plasma observations Atrsophys. J. Letter, 246, L165-169, 1981.

Mewaldt, R.A., E.L. Stone, and R.E. Vogt, Characteristics of the spectra of protons and Alpha particles in recurrent events at 1 AU, Geophys. Res. Lett., 6, 589-593, 1980.

Ogilvie, K.W. and J.F. Arens, Acceleration of protons by interplanetary shocks, J. Geophys. Res., 76, 13-18, 1971.

Palmeira, R.A., F.R. Allum, and U.R. Rao, Low-Energy proton increases associated with interplanetary shock waves, Sol. Phys., 21, 204-224, 1971.

Pesses, M.E., Energetic proton events observed between 1 and 5 AU by Pioneer 11, M.S thesis, University of Iowa, Iowa City, 1976.

Pesses, M.E., The acceleration of ions by interplanetary shock waves: 1, Single encounter considerations, submitted to J. Geophys. Res., 1982.

Pesses, M.E. and Decker, R.B. The acceleration of ions by interplanetary shock waves: 2, Multiple encounter considerations, submitted to J. Geophys. Res., 1982.

Pesses, M.E., B.T. Tsurutani, J.A. Van Allen, and E.J. Smith, Acceleration of energetic protons by interplanetary shocks, J. Geophys., Res., 84, 7297-7301, 1979.

Potter, D., Acceleration of Electrons by Interplanetary Shocks, Submitted to J. Geophys. Res., 1981.

Rao, U.R., K.G. McCracken, and R.P. Bukata, Cosmic ray propagation process. 2. The energetic storm-particle event, J. Geophys. Res., 72, 4325-4341, 1967.

Sarris, E.T., Effects of interplanetary shock waves on energetic charged particles, Ph.D. thesis, University of Iowa, Iowa City, 1973.

Sarris, E.T., S.M. Krimigis, and T.P. Armstrong, Observations of energetic particles near interplanetary MHD discontinuities, Proc. 14th International Cosmic Ray Conference, 5, 1835-1840, 1975.

Sarris, E.T., S.M. Krimigis, and T.P. Armstrong, Observations of high energy ion shock spikes in interplanetary space, Geophys. Res. Lett., 2, 133-136, 1976.

Sarris, E.T. and J.A. Van Allen Effects of interplanetary shock waves on energetic charged particles, J. Geophys. Res., 79, 4157-4173, 1974.

Singer, S., The association of energetic storm particles with interplanetary shock waves, in Intercorrelated Satellite Observations Related to Solar Events, ed. by V. Manno and D.E. Page, pp 571-582, D. Reidel, Dordrecht-Holland, 1970.

Smith, E.J., B.V. Connor, and G.T. Foster, Jr. Measuring the magnetic field of Jupiter and the outer solar system, IEEE Trans. Magn., MAG-11, 962-980, 1975.

Tsurutani, B.T., E.J. Smith, D.L. Chenette, T.F. Conlon, K.R Pyle, and J.A. Simpson, Energetic protons accelerated at contracting shocks: Pioneer 10 and 11 observations from 1-b AU, Submitted to J. Geophys. Res., 1981.

Van Allen, J.A. and N.F. Ness, Observed particle effects of an interplanetary shock wave, J. Geophys. Res., 72, 935-942, 1967.

Van Allen, J.A. and W.H. Whelpley, Radation observations with satellite Injun 1, September 28 - October 4, 1971, J. Geophys. Res., 67, 1660-1661, 1962.

Van Hollebeke M.A.I., F.B. McDonald, J.H. Trainor, and T.T. Von Rosenvinge The radial variation of corotating energetic particle streams in the inner and outer solar system, J. Geophys. Res., 83, 5001-5019, 1978.

Van Hollebeke, M.A.I., F.B. McDonald, J.H. Trainor, and T.T. Von Rosenvinge, Corotating energetic particle and fast plasma streams in the inner and outer solar system - radial dependence and energy spectra, to be published in The Solar Wind 4 Conference Proceedings, in Lecture Notes in Physics, ed. by P. Berblbock, 1981.

Vernov, S.N., A.E. Chudakov, P.V. Vakulov, E.V. Gorchakov, N.N. Kontor, Yu. I. Logachev, N.V. Pereslegina, and G.A. Timofeev, Propagation of solar and galactic cosmic rays of low energies in interplanetary medium, in Intercorrelated Satellite Observations Related to Solar Events, ed. by V. Manno and D.E. Page, p. 53, D. Reidel, Dordrecht-Holland, 1970.

Wolfe, J.H., J.D. Mihalov, H.R. Colland, D.D. McKibben, L.A. Frank, D.S. Intriligator, Pioneer 10 observations of the solar wind interaction with Jupiter, J. Geophys. Res., 79, 3489-3500, 1974.

Table 1

Characteristics of Selected University of Iowa

Detectors on Pioneer 11

Detector	Energy Range, MeV		Inverse Geometric Factors	
	Protons	Electrons	Protons	Electrons
G	$0.61 \leq E_p \leq 3.41$	[*]	24.7	... $(cm^2 sr)^{-1}$
A - C	$0.61 \leq E_p \leq 80$	$0.047 \leq E_e \leq 21$	50.8	58.9 $(cm^2 sr)^{-1}$
B - C	$9 \leq E_p \leq 80$	$0.56 \leq E_e \leq 21$	51.7	66.1 $(cm^2 sr)^{-1}$
C	$E_p > 80$	$F_e > 21$	8.2	23 cm^{-2}

LIST OF FIGURES

Figure 1. Schematic view of spacecraft observation of shock accelerated particle process.

Figure 2. The CIR shock associated event of DOY 238/1973.

Figure 3. The CIR shock associated event of DOY 163/1973.

Figure 4. The CIR shock associated event of DOY 103/1974.

Figure 5. The CIR shock associated event of DOY 166/174.

Figure 6. The CIR shock associated event of DOY 329/1973 (minute averages).

Figure 7. The CIR shock associated event of DOY 302/1974.

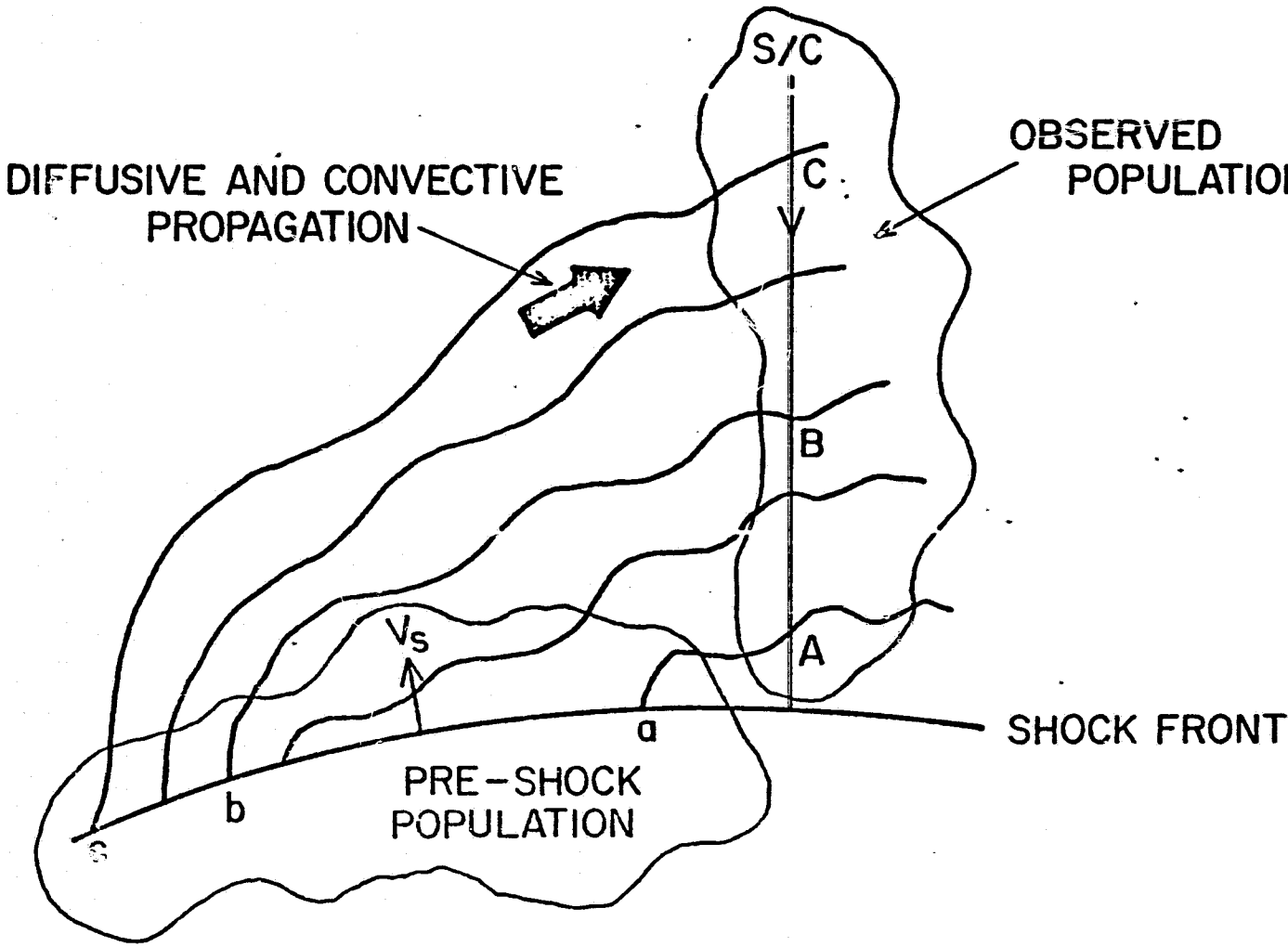

Figure 1

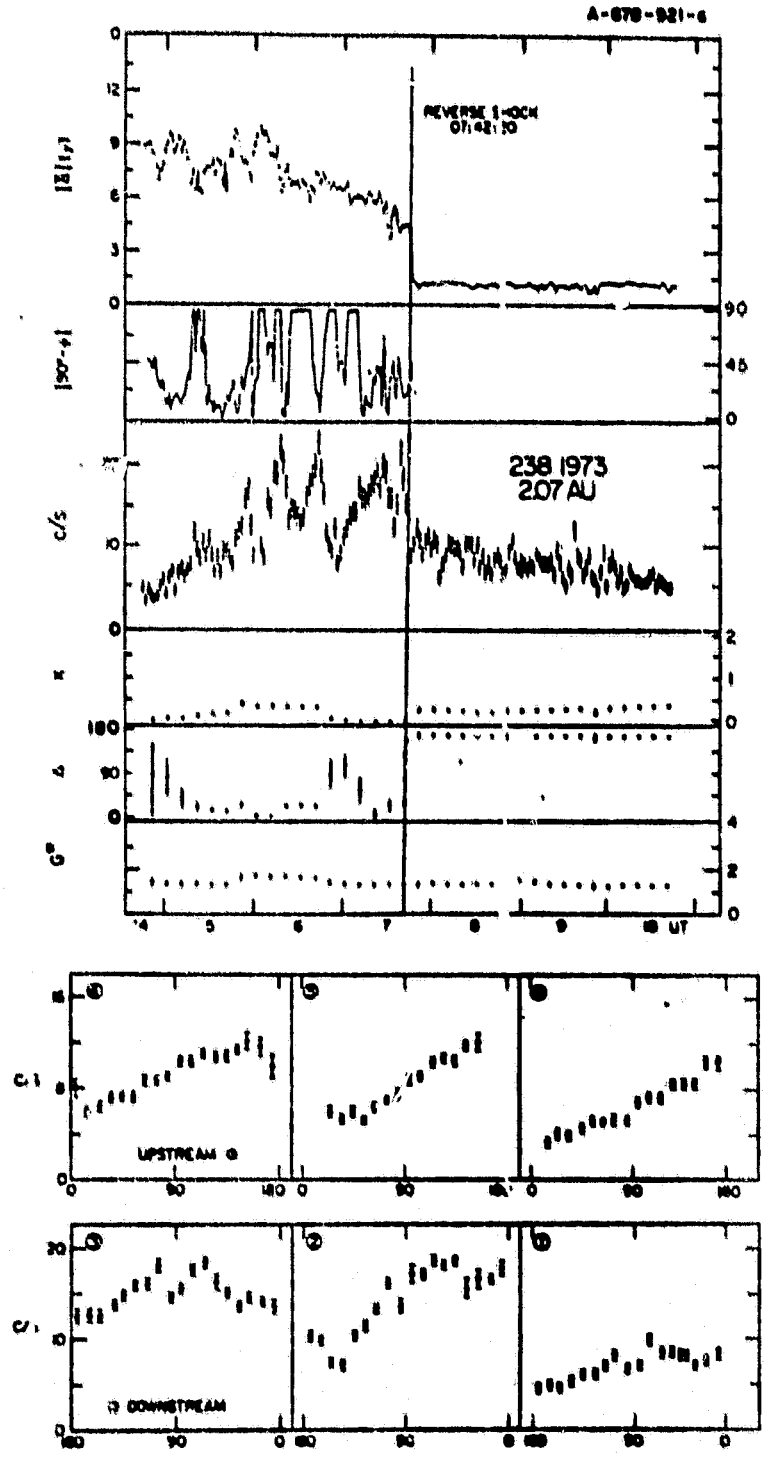

Figure 2

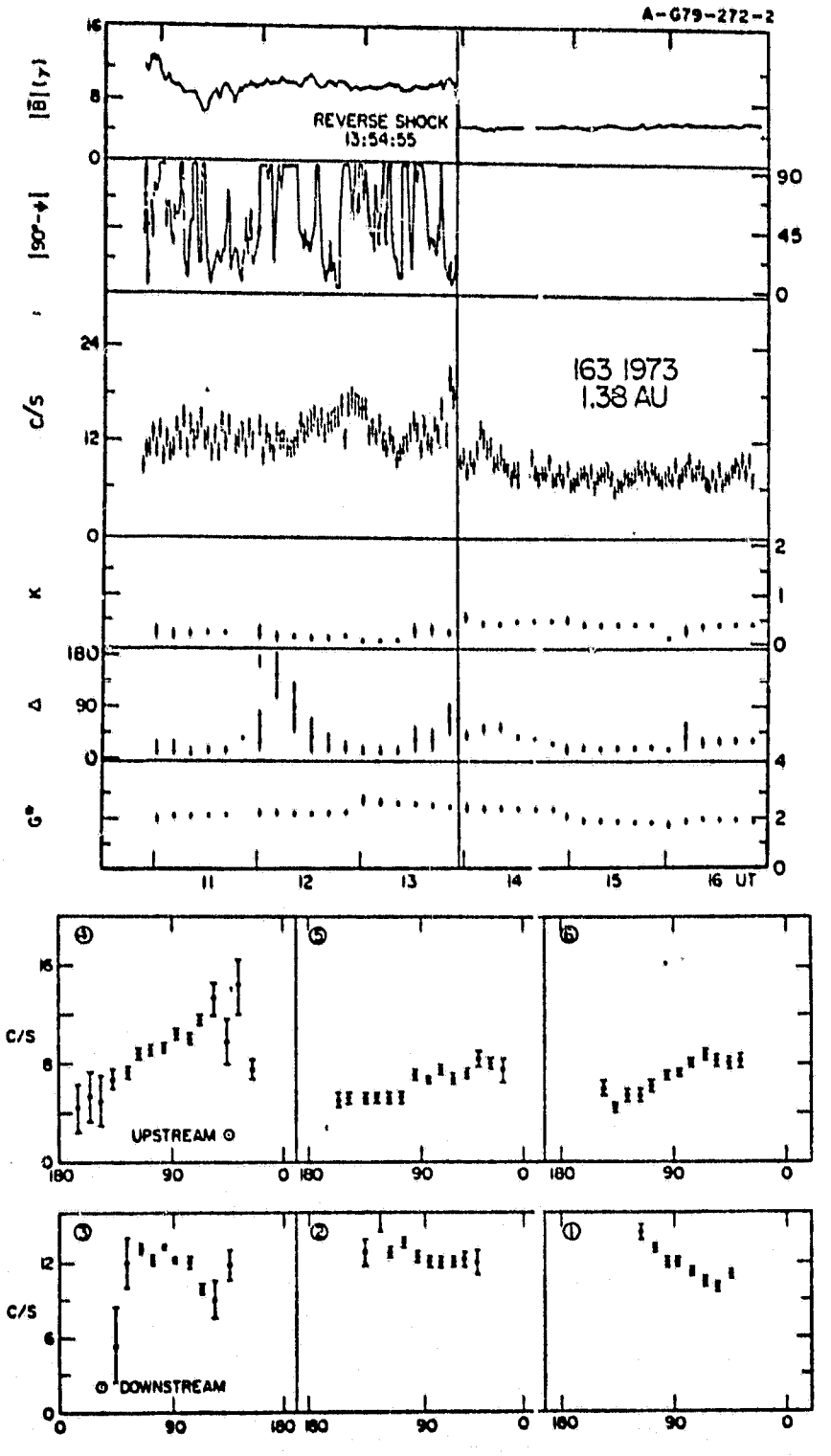

Figure 3

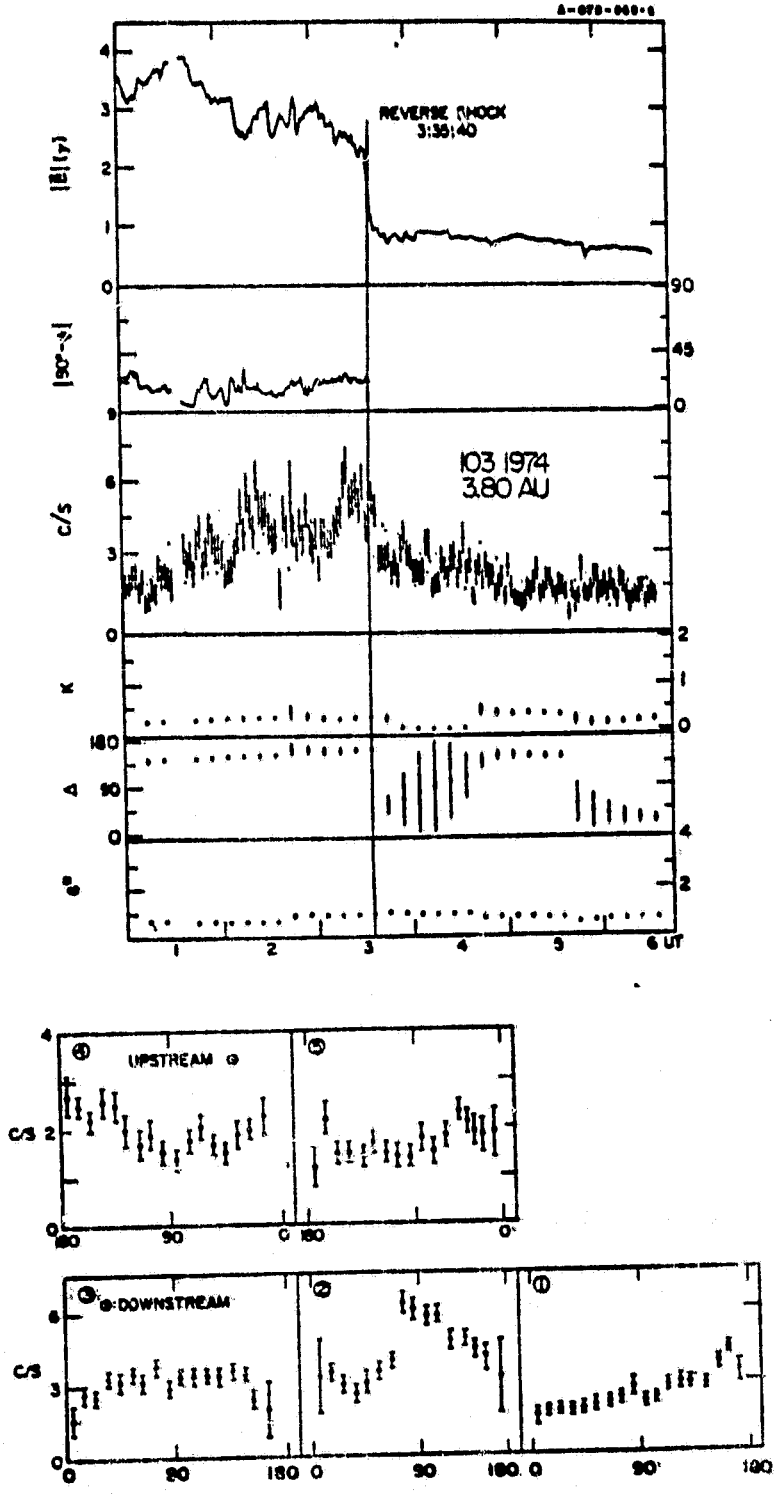

Figure 4

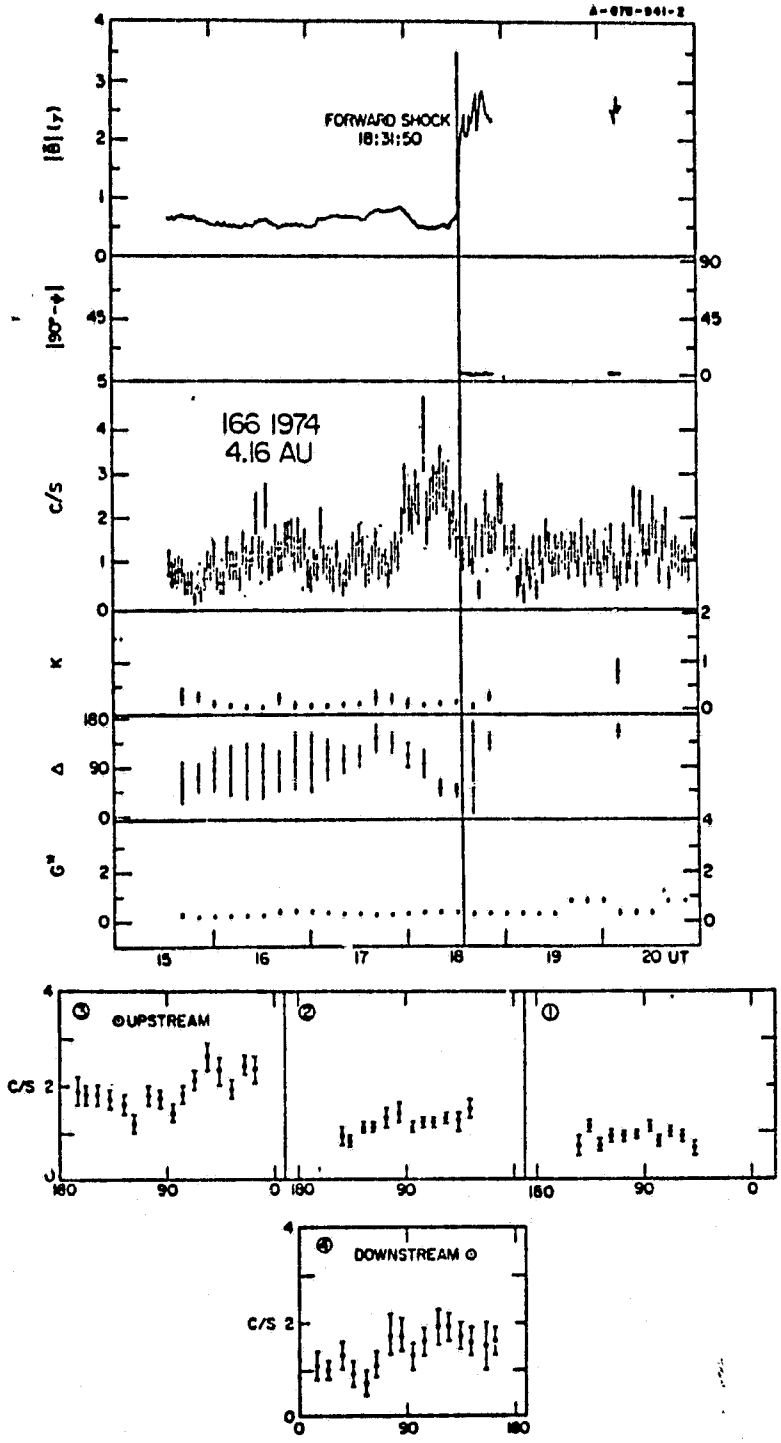

Figure 5

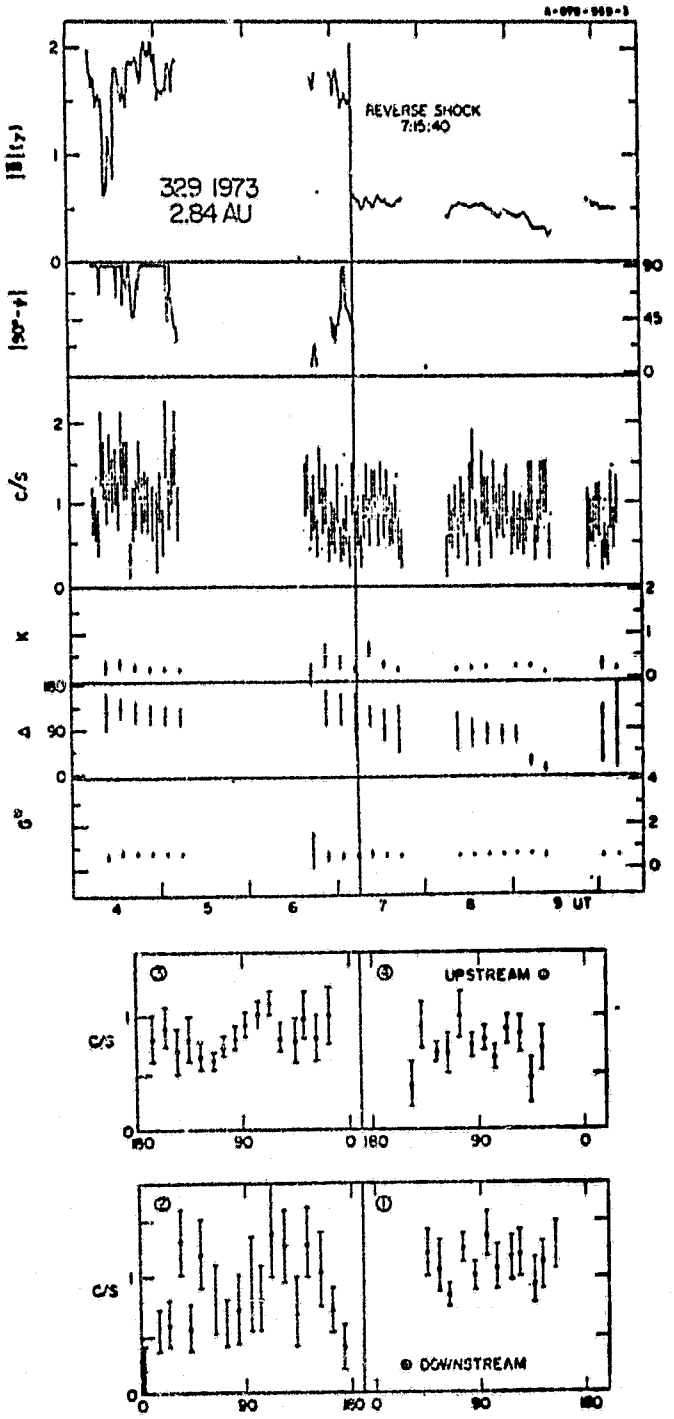

Figure 6

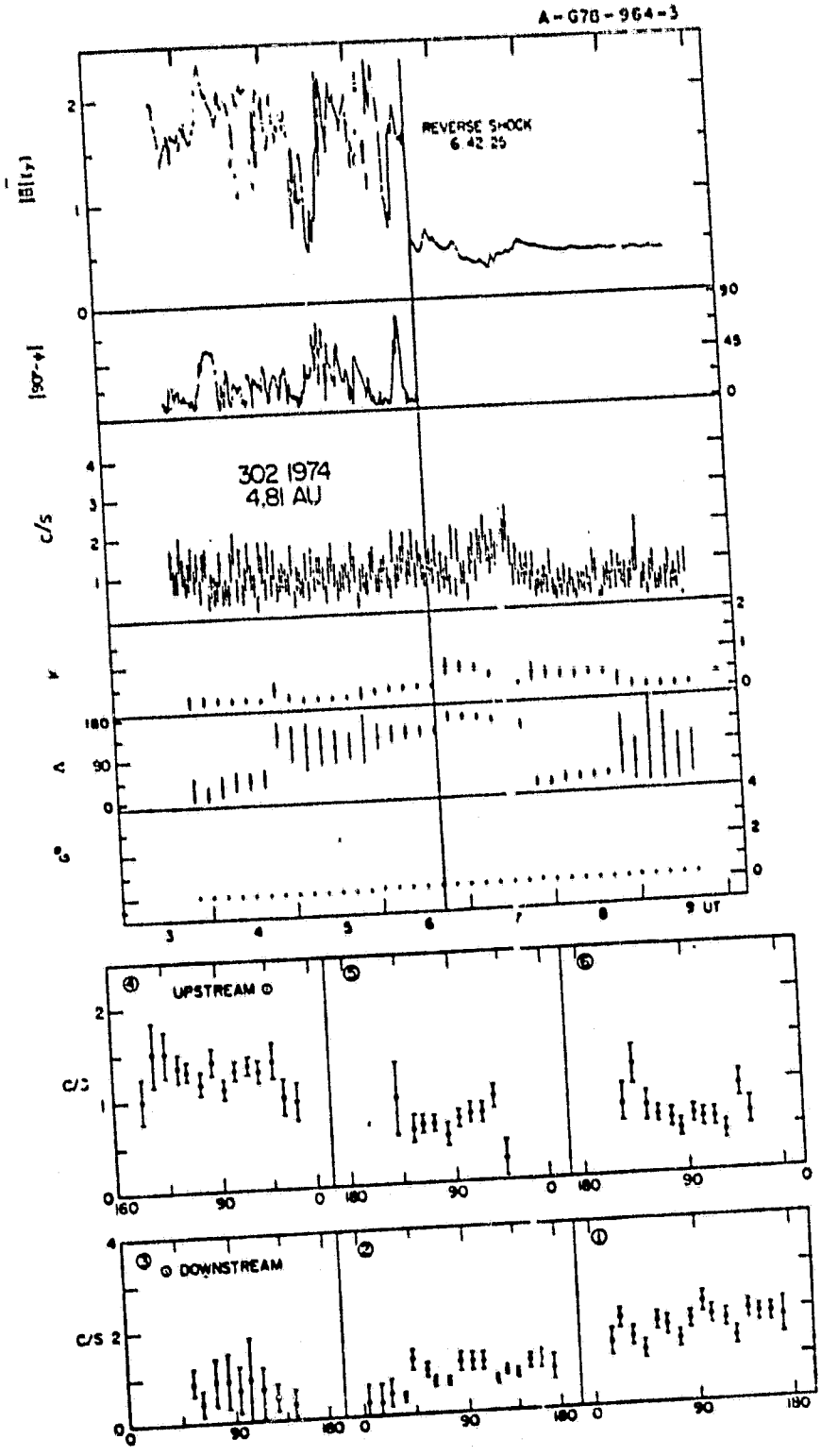

Figure 7